Submitted to
Europhysics Conference on High Energy Physics, EPS2007, July 19-25, 2007, Manchester
Abstract: **237**
Parallel Session **Strong Interactions**
Electronic Access: www-h1.desy.de/h1/www/publications/conf/conf_list.html

Measurement of the Inclusive ep Scattering Cross Section at low Q^2 and high y at HERA

H1 Collaboration

Abstract

A new preliminary measurement of the inclusive ep scattering cross section from H1 experiment at HERA is presented in the region of low four-momentum transfer squared, 12 GeV $^2 < Q^2 < 50$ GeV^2 and very high inelasticity, $0.75 < y < 0.9$. The cross section in this kinematic domain is sensitive to the longitudinal structure function F_L and thus provides additional constraints to the DGLAP evolution. The results are based on data collected in 2003-2006 (HERA-II). About equal luminosities obtained for e^+p and e^-p collisions allow for a high precision control of background processes.

1 Introduction

The $e^{\pm}p$ deep-inelastic scattering (DIS) double-differential cross section at low values of squared four momentum transfer, Q^2, in the one-photon exchange approximation, can be expressed as,

$$\frac{d^2\sigma}{dxdQ^2} \cdot \frac{Q^4 x}{2\pi\alpha^2 Y_+} = \sigma_r = F_2(x,Q^2) - \frac{y^2}{Y_+} \cdot F_L(x,Q^2) \ , \tag{1}$$

where x is the Bjorken scaling variable, $y = Q^2/sx$ is the inelasticity which is a fraction of the electron's[1] energy loss, s is the center of mass energy squared of the electron-proton system and $Y_+ = 1 + (1-y)^2$. The two structure functions F_2 and F_L obey the relation $0 \leq F_L \leq F_2$ due to the positivity of the cross sections for transversely and longitudinally polarised photons scattering off protons. Therefore, the longitudinal structure function, F_L, gives a sizable contribution to the cross section only at large values of the inelasticity y. The longitudinal structure function, F_L, is identically zero in lowest order QCD, but due to gluon radiation gets a non-zero value in perturbative QCD. The measurement of F_L can thus provide constraints on the gluon density function which are complementary to those obtained from the scaling violations of F_2 assuming DGLAP evolution [1].

The new high y cross section measurement from H1 is based on HERA-II data with integrated luminosity of 96 pb^{-1} where 51 pb^{-1} is from e^+p and 45 pb^{-1} from e^-p interactions. Lepton beam energy is 27.5 GeV and proton beam energy is 920 GeV. The kinematic plane covered in this analysis is shown in figure 1 together with kinematic planes from the analysis of HERA-I data from H1 and fixed target experiments.

2 Principle of the measurement

2.1 Kinematic Reconstruction

DIS kinematics can be reconstructed using the scattered electron, the hadronic final state, or a combination of the two. At high y the event kinematics is best determined using the measured energy of the scattered electron, $E_e{}'$, and its polar angle, θ_e, (electron method) according to the relations

$$y = 1 - \frac{E_e{}'}{E_e}\sin^2(\theta_e/2), \qquad Q^2 = \frac{E_e{}'^2 \sin^2\theta_e}{1-y}. \tag{2}$$

Thus, to measure at largest values of y, it is necessary to reach as low as possible $E_e{}'$.

Due to energy and longitudinal momentum conservation the variable

$$E - p_z = \Sigma_i(E_i - p_{z,i}) + E_e{}'(1 - \cos\theta_e) \tag{3}$$

[1]The name *electron* in the text is used to denote both electrons and positrons.

is approximately equal to $2E_e$ where E_e is electron beam energy. E_i and $p_{z,i}$ are the energy and longitudinal momentum component of a particle i in the hadronic final state, the masses being neglected.

The scattered electron energy and the polar angle is measured in the backward electromagnetic lead scintillating fibre calorimeter (spaghetti calorimeter - SpaCal) [2]. The hadronic final state is reconstructed in the Central Tracker, Liquid Argon calorimeter and the SpaCal [3].

2.2 Event Selection

To select events with low and medium Q^2 with the H1 detector at least one cluster in SpaCal is required. Copious photoproduction processes often lead to electron-like low energy deposits in SpaCal. Thus the high level of the photoproduction background is the main difficulty for a cross section measurement at large values of y. A sizable background of hadrons originates also from deep inelastic scattering because at high y and low Q^2 the hadronic final state is scattered backwards. Electromagnetic energy deposition leads to clusters of smaller transverse extension than hadronic energy deposition. Thus to suppress hadronic contributions, cuts on the shower shape estimators are performed. Also any energy behind the electron cluster measured in the hadronic SpaCal may not exceed a small fraction of $E_e{}'$. An additional suppression of the radiative events and photoproduction background is performed by requiring energy and longitudinal momentum conservation. A well reconstructed vertex is required in the interaction region to further reduce background and contribution from beam gas interactions. The cuts were optimized to avoid efficiency loss as much as possible and to still significantly reduce background.

The high level of the background at large values of y leads directly to an additional uncertainty in the background subtraction procedure. The background also complicates the estimation of the signal selection efficiency in an unbiased way. To achieve an efficient rejection and identification of photoproduction background, this analysis does not rely on the Monte Carlo simulation for the background level estimation, but uses experimental information by employing the charge assignment of central tracks associated with SpaCal energy cluster. The sample of candidates with negative charge is taken to represent the background in the positron data sample and vice versa. This allows the energy range to be extended down to 3.4 GeV corresponding to $y \leq 0.9$.
The criteria applied to select DIS events are summarised in table 1.

The efficiency of the high y first level trigger used in the analysis is uniform in radius and energy in SpaCal and is about 97 $\%$ for the total data sample.

2.3 Background Estimation

The charge of central track associated with SpaCal cluster is determined from the sign of ratio of its energy and momentum (energy is measured from SpaCal and momentum from the central tracking chambers). Figure 2 shows the energy over momentum ratio from e^+p interactions for tracks which pass all the cuts and are linked to clusters with energy from 3.4 GeV to 10 GeV. The

SpaCal energy	> 3.4 GeV
radius of cluster	< 5 cm
fraction of energy in the hadronic section	$< 15\ \%$ of $E_e{}'$
cluster-central track link	< 6 cm
z-vertex position	$\|z\| < 35$ cm
$E - p_z$ cut	> 27.5 GeV

Table 1: Basic DIS event selection criteria.

smaller peak corresponds to tracks with negative charge and is almost a pure background with a charge misidentification probability about 0.5 $\%$. These tracks are termed as wrong sign tracks. The higher peak, near $E/p = 1$, contains signal plus remaining positive background (correct sign tracks). The statistical subtraction procedure requires the study of any process which may cause a charge asymmetry. The charge asymmetry of the background can arise from the charge of the incident proton (small effect) and from reconstruction biases. In particular, tracking chambers can have different efficiency for positive and negative tracks due to asymmetric jet-geometry. Also calorimetry may have different response to charged hadrons (e^+ vs e^- cross section differences are negligible for this analysis). Monte Carlo studies show that the positively and negatively charged pions and kaons lead to similar responses in the calorimeter, while for protons and anti-protons there is a significant difference. Protons, having smaller kinetic energy compared to pions, tend to produce smaller energy deposits. Anti-protons, on the other hand, having larger interaction cross sections and release additional energy due to annihilation, deposit more than pions on average. The final state photon and the electron, scattered at very low Q^2, can be detected in calorimeters ("electron and photon tagger") which are situated close to the beam pipe in the electron beam direction. Thus, background charge asymmetry can be measured using tagged photoproduction events which fulfill the DIS even selection criteria. A small charge asymmetry, N_-/N_+ is found with an average 1.057 ± 0.009. N_+ (N_-) is the number of events with positive (negative) charge of the track associated with the SpaCal cluster. Comparing distributions for a sample of negative tracks in e^+p scattering with that for a sample of positive tracks in e^-p scattering , a consistent asymmetry of 1.062 ± 0.007 is measured.

Other analysis details like alignment and calibration of the detector can be found elsewhere [6].

2.4 Control Plots

A high statistics simulation of DIS events is performed using the program DJANGO [5]. The simulation of the DIS cross section uses a QCD parameterisation of the structure functions [7] which in an iterative process has been adjusted to the measured cross section.
Figure 3 shows the comparison of data and MC distributions for energy of scattered electron, polar angle of scattered electron, z-coordinate of vertex and $E - p_z$ for the combined charge symmetrized[2] sample. For all distributions the background contribution in data is estimated using wrong charge events and is shown as shaded histogram. The DIS MC simulation corresponds to correct sign events with a small contribution from the wrong sign events subtracted.

[2]The e^- data sample was scaled to the luminosity of the e^+ sample, then both samples were added.

Source	Uncertainty of the Source	Effect on the Cross section
Tracking efficiency	1.5%	1.5%
Trigger efficiency	1.2%	1.2%
Track charge determination	0.5%	1.0%
Electron identification	0.5%	0.5%
E'_e energy scale	1% at 2 GeV and 0.2% at 27.5 GeV	$\sim 0.5\%$
SpaCal alignment	1 mrad	$\sim 0.5\%$
SpaCal $E - p_Z$	± 1 GeV	$\sim 0.8\%$
LAr Scale	3%	$\sim 0.1\%$

Table 2: Systematic uncertainties in the high y analysis, size and impact on the cross section measurement.

The sum of background and signal MC is shown as an open histogram. The plots correspond to a range in the scattered electron energy $3.4 < E'_e < 10$ GeV. All plots are luminosity normalized. A comparison for the corresponding background subtracted distributions is shown in figure 4. The direction of arrows in the figures points to the region rejected by the cut.

Figure 5 shows a comparison of the correct sign data (dots) with a sum of background determined from the wrong sign data (shadowed histogram) and DIS Monte Carlo simulation for y, Q^2 and x distributions. A comparison for the corresponding background subtracted distributions is shown in Figure 6. As can be seen from these figures, data are well described by Monte Carlo simulation.

2.5 Systematic Uncertainties

The systematic uncertainty of the new measurement is 2-3 $\%$ and is dominated by the track link efficiency uncertainty which is estimated to be 1.5 $\%$. Other sources of uncorrelated systematic uncertainties are: trigger efficiency (1.2 $\%$), track charge identification (0.5 $\%$) and electron identification (0.5 $\%$). Concerning correlated errors, the main influence comes from the $E_e{}'$ energy scale uncertainty (1 $\%$ at 3 GeV), the θ_e uncertainty (1 mrad) and the calorimeter hadronic energy scale uncertainty ($\pm$ 1 GeV).
The overall summary of the uncertainties, size and impact on the cross section measurement is given in table 2.

3 Results

A very sensitive cross check of the analysis is the comparison of the double differential cross section measured using e^+ and e^- beam periods separately. The two measurements are sensitive to the background charge asymmetry and also different systematic effects appeared during the data taking. Figure 7 shows this comparison along with the cross section measurement using the charge symmetrized sample for inelasticity $y = 0.825$. Only statistical errors are shown. The bottom panel of figure 7 shows the ratio of e^+ over e^- cross sections also with statistical errors. The charge symmetrized cross section measurement, as expected, appears in between

the measurements with the different charges. The charge symmetrized measurement is used for the new preliminary result.

Figure 8 compares the new preliminary cross section depending on Q^2 at inelasticity $y = 0.825$ with the published H1 result based on HERA-I data [6, 7]. The new measurement has significantly reduced uncertainties. The total uncertainty is reduced by about factor of two. Unlike for the published H1 result, based on HERA-I data, for this analysis a large sample of data from e^-p interactions is available for cross section measurement and the control of the charge asymmetry which provides much improved understanding of systematics. The published data corresponds to a slightly lower center of mass energy[3]. The overall luminosity error, which is not included in the figures, is estimated to be $\sim 2\%$.

Figure 9 compares the measurement presented in this note (dots) with other H1 measurements: a combination of preliminary minimum bias 97 data, minimum bias 99 data and shifted vertex 2000 data (triangles) [8], and measurement from 97 data for $y < 0.6$ (squares). The line is H1 QCD fit [7].

4 Summary

A double differential cross section measurement at high inelasticity, $y = 0.825$, is obtained using data from HERA II collected with the H1 apparatus. Integrated luminosity of the data corresponds to 96 pb^{-1} where 51 pb^{-1} is from e^+p and 45 pb^{-1} from e^-p interactions.

Double differential cross section measurements obtained separately from e^+p and e^-p interactions are compared and are consistent. This is an important cross check since the two measurements are sensitive to the background charge asymmetry and to the different systematic effects.

The precision of the new measurement is about factor of 2 better than in published measurements from H1 (97 data) for the highest y with the same Q^2 range. Still, the precision can be improved, mainly with regard to the tracking efficiency which is a dominant systematic error source, by exploiting the Backward Silicon Tracker (BST) [4] in the kinematic region which overlaps with central tracking chambers. This work is in progress.

This analysis shows that at H1 there are advanced tools to cope with a large background at low energies which is vital for the direct accurate measurement of the longitudinal structure function as is expected to be derived from the HERA low proton energy run data.

Acknowledgements We are grateful to the HERA machine group whose outstanding efforts have made this experiment possible. We thank the engineers and technicians for their work in constructing and maintaining the H1 detector, our funding agencies for financial support, the DESY technical staff for continual assistance and the DESY directorate for support and for the hospitality which they extend to the non DESY members of the collaboration.

[3] the published data corresponds to the proton energy of Ep=820 GeV.

References

[1] V. Gribov and L. Lipatov, Sov. J. Nucl. Phys. **15**, 438 and (1972) 675; L. Lipatov, Sov. J. Nucl. Phys. **20**, (1975) 94; G. Altarelli and G. Parisi, Nucl. Phys. B **126**, (1977) 298; Y. Dokshitzer, Sov. Phys. JETP , (1977) 641.

[2] R. Appuhn *et al.*, Nucl. Instr. and Meth. **A386** (1996) 397.

[3] H1 Collaboration, I. Abt *et al.*, Nucl. Instr. and Meth. **A386** 310 and **A386** (1997) 348.

[4] V.V. Arkadov, PhD Thesis, Berlin, Humboldt-University, 2000, DESY-Thesis-2000-046; D. Eckstein, PhD Thesis, Berlin, Humboldt-University, 2002, DESY-Thesis-2002-008; T. Laštovička, PhD Thesis, Berlin, Humboldt-University, 2004, DESY-Thesis-2004-016.

[5] G.A. Schuler and H. Spiesperg, Proc. Workshop on HERA Physics, Vol 3, eds. W. Buchmuller and G. Ingelman, Hamburg, DESY (1992), p. 1419; A. Kwiatkowski, H. Spiesberg and H.-J. Mohring, Comp. Phys. Comm. **69** (1992) 155; L. Lonnblad, Comp. Phys. Comm. **71** (1992) 15.

[6] A.A. Glazov, PhD Thesis, Berlin, Humboldt-University, 1998, DESY-Thesis-1998-005.

[7] H1 Collaboration, C. Adloff *et al.*, Eur. Phys. J. **C19**, (2001) 269.

[8] H1 Collaboration, Conference note for EPS07, abstract 234.

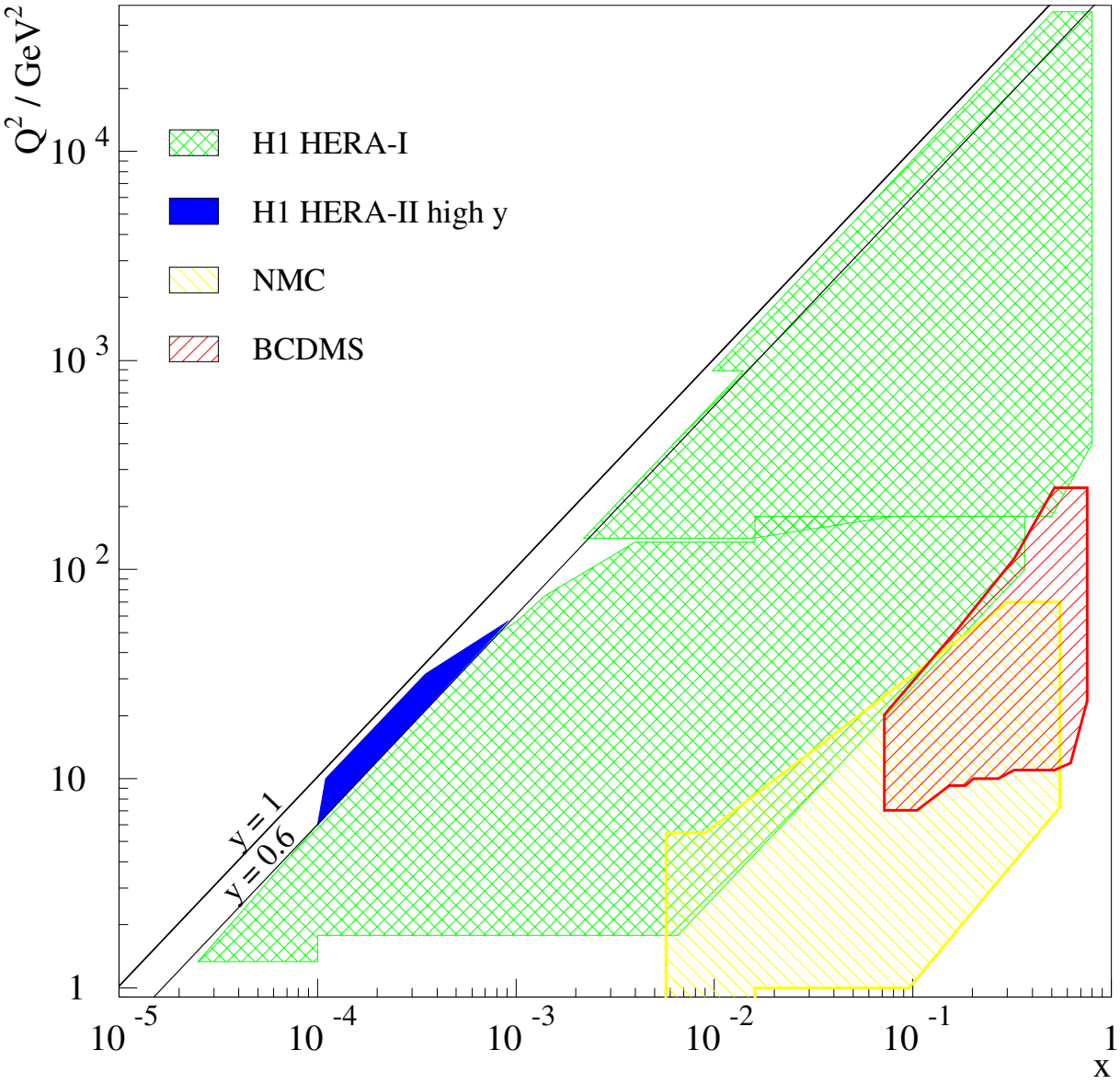

Figure 1: Kinematic plane covered by H1 and fixed target experiments. Dark region, labeled H1 HERA-II high y, corresponds to this analysis.

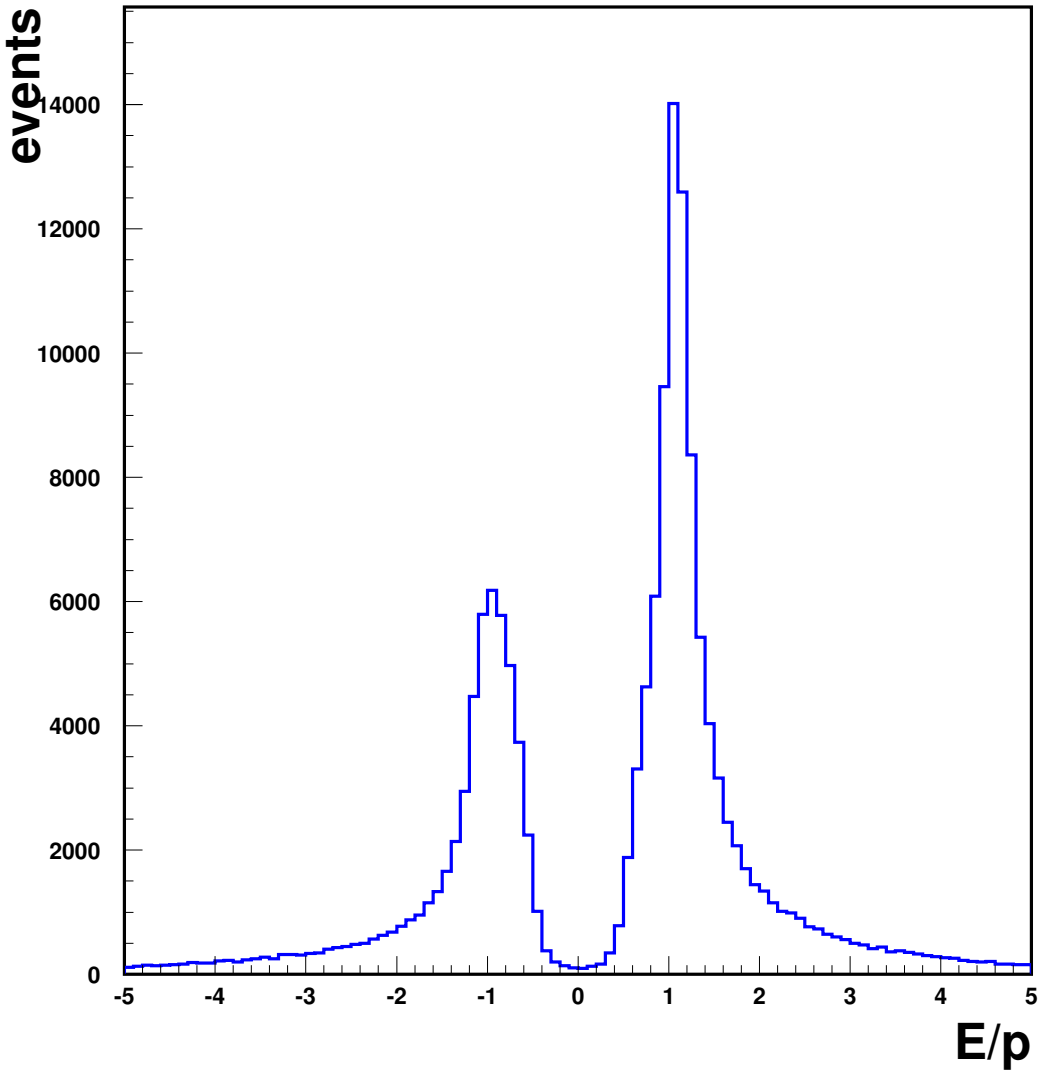

Figure 2: Energy over momentum for tracks from e^+p interactions linked to clusters in SpaCal with energy from 3.4 to 10 GeV which pass all the cuts listed in table 1.

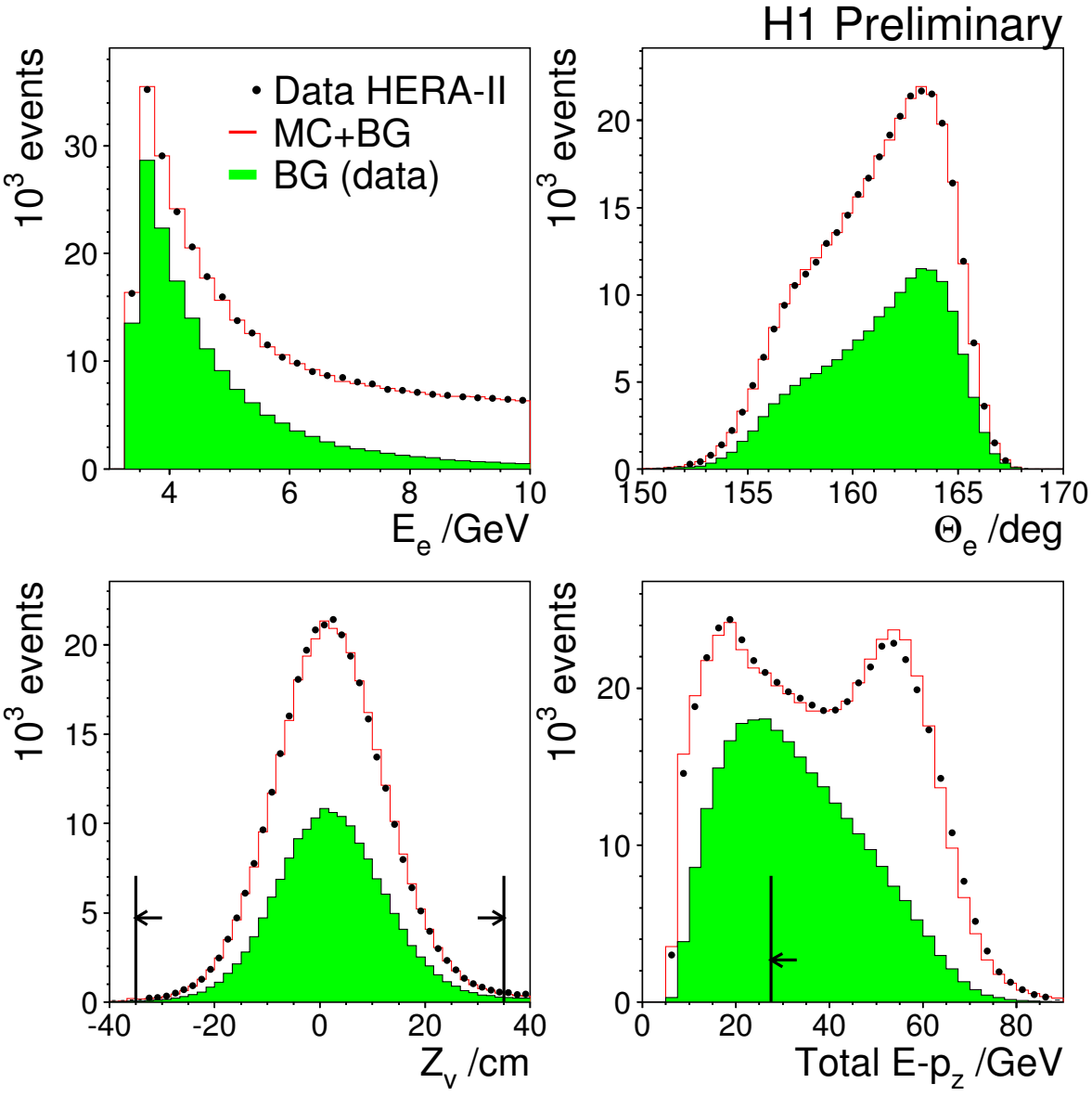

Figure 3: Comparison of the correct sign data (dots) with a sum of background determined from the wrong sign data (shadowed histogram) and DIS Monte Carlo simulation (open histogram) for energy of the scattered electron, polar angle of the scattered electron, z-coordinate of central vertex and $E - p_z$ distributions. Arrows point to the regions rejected by the cut.

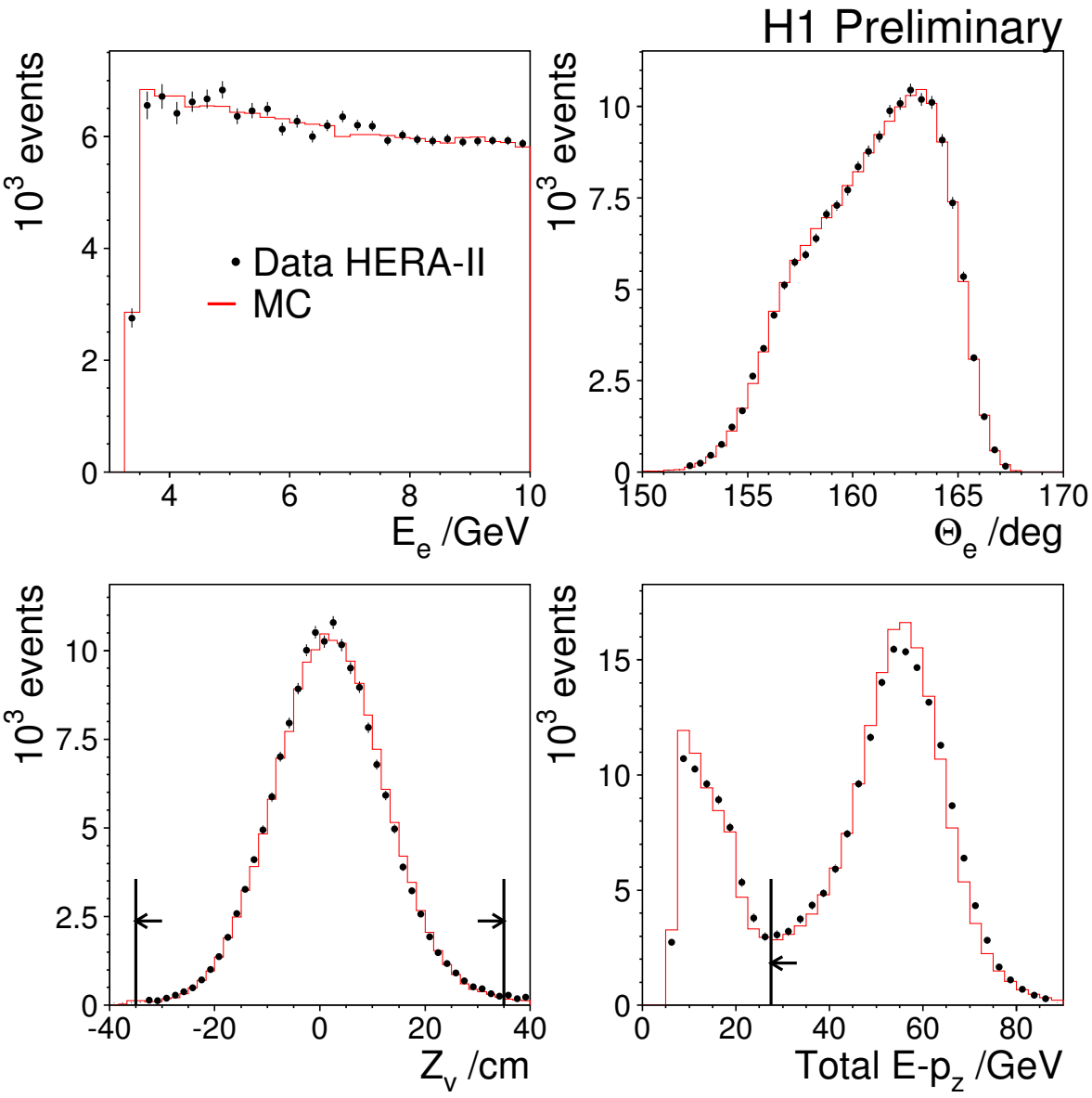

Figure 4: Comparison of the background subtracted data (dots) and DIS Monte Carlo simulation (histogram) for energy of the scattered electron, polar angle of the scattered electron, z-coordinate of central vertex and $E - p_z$ distributions. Arrows point to the regions rejected by the cut.

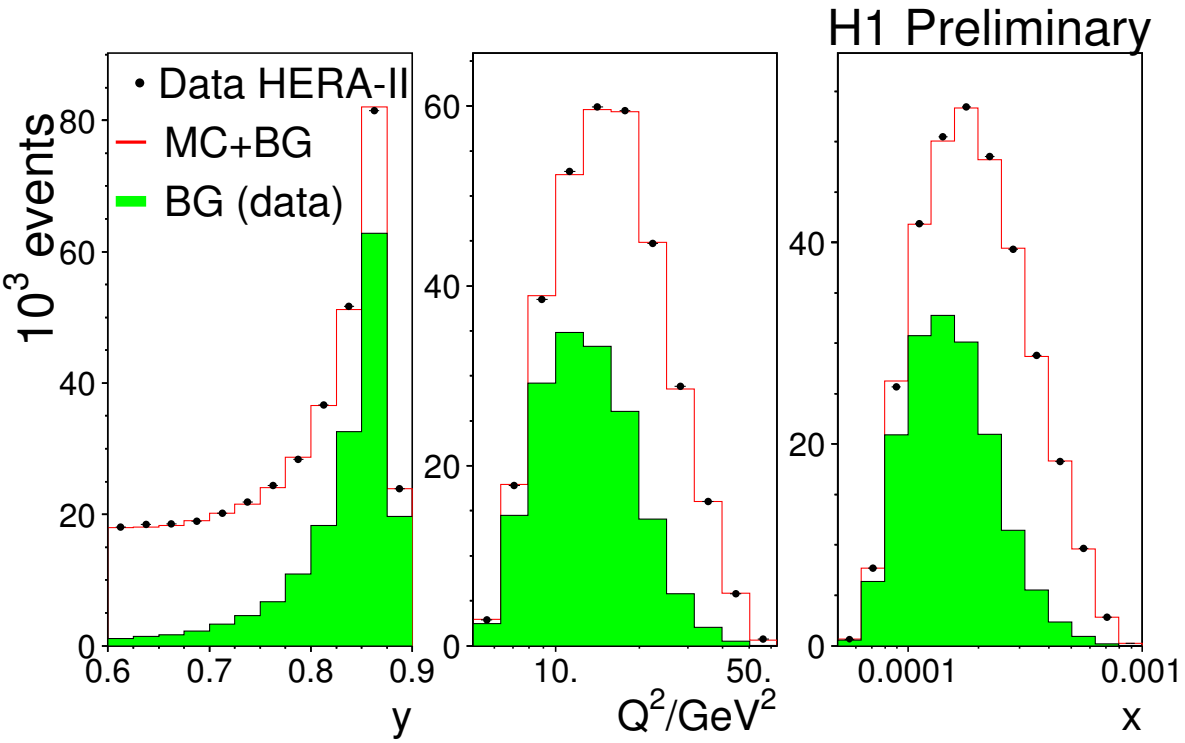

Figure 5: Comparison of the correct sign data (dots) with a sum of background determined from the wrong sign data (shadowed histogram) and DIS Monte Carlo simulation for y, Q^2 and x distributions (open histogram).

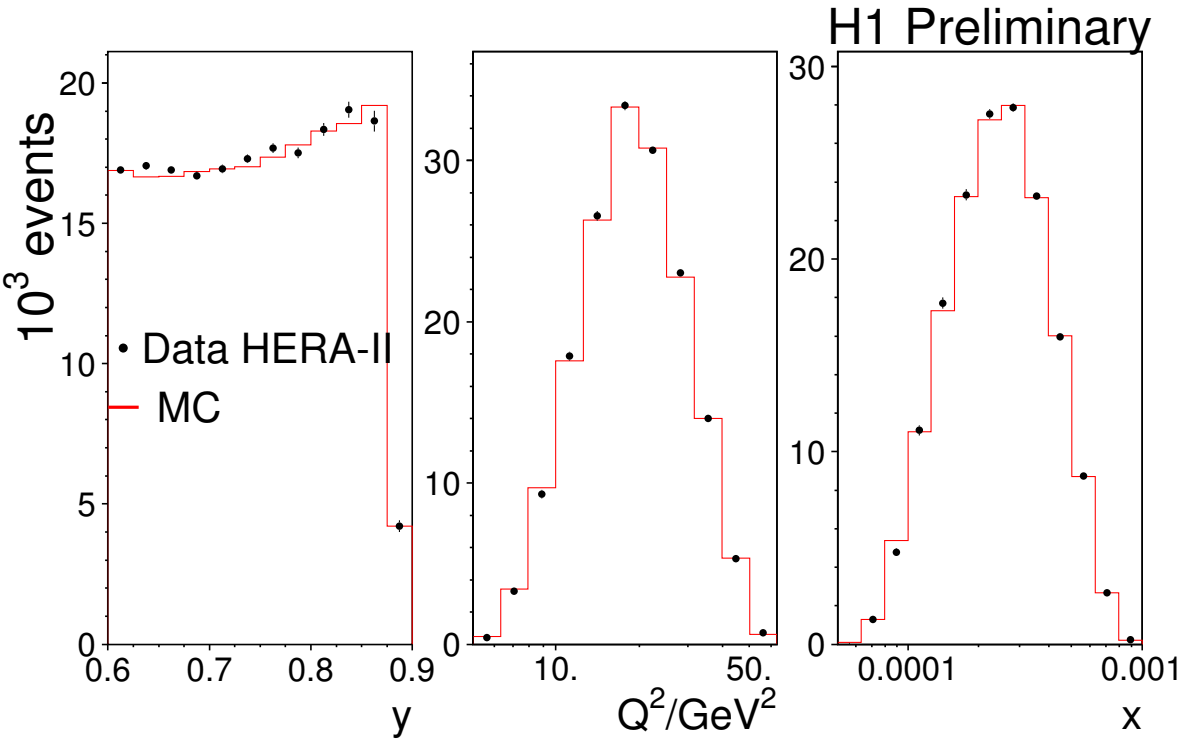

Figure 6: Comparison of the background subtracted data (dots) and DIS Monte Carlo simulation (histogram) for y, Q^2 and x distributions.

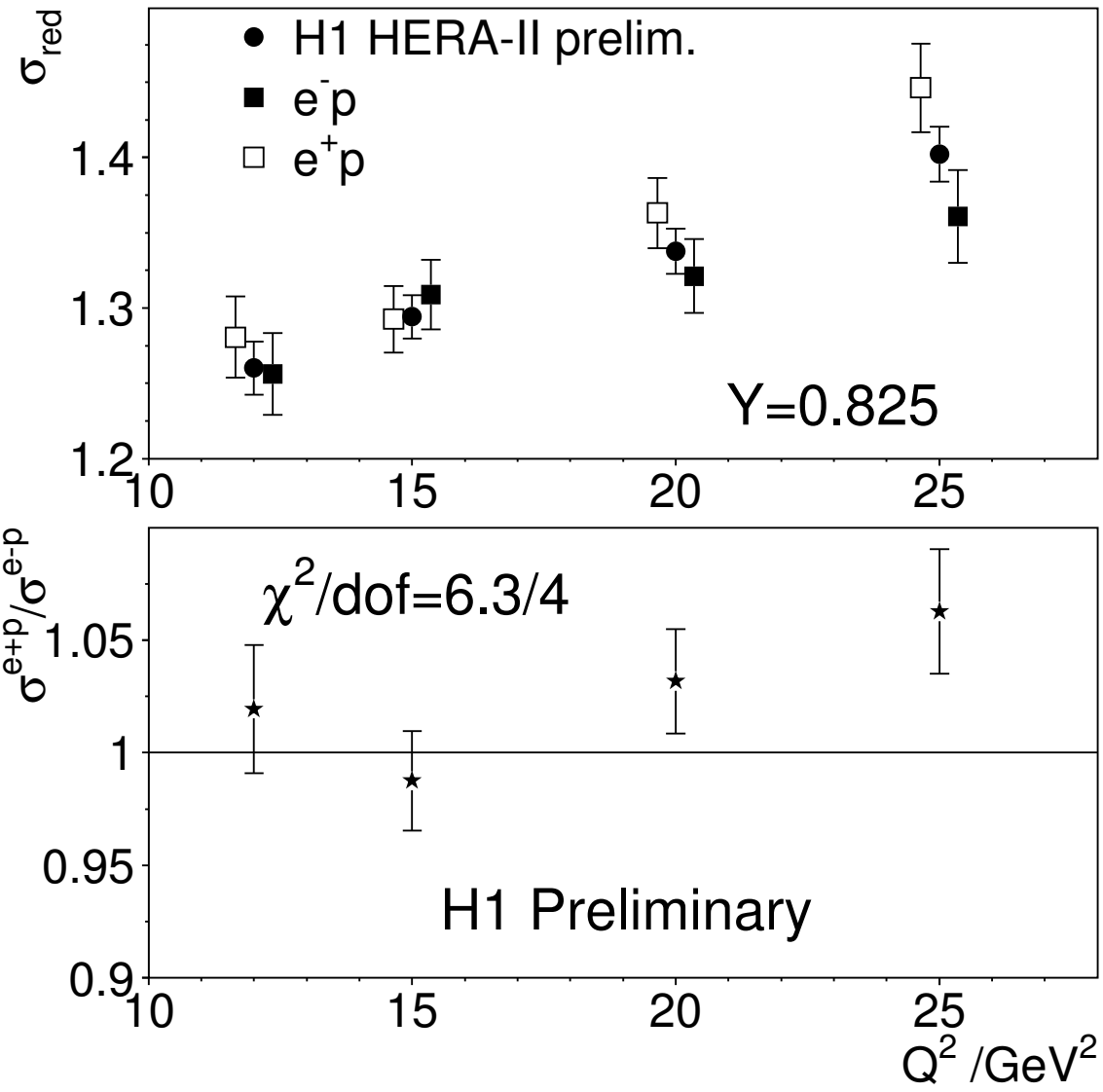

Figure 7: Top: Q^2 dependence of the reduced cross section measured for e^-p (black squares) and e^+p (open squares) data for inelasticity $y = 0.825$. Cross section measurement obtained using charge symmetric sample is shown by dots. Bottom: Ratio of the e^+ to e^- cross section measurements.

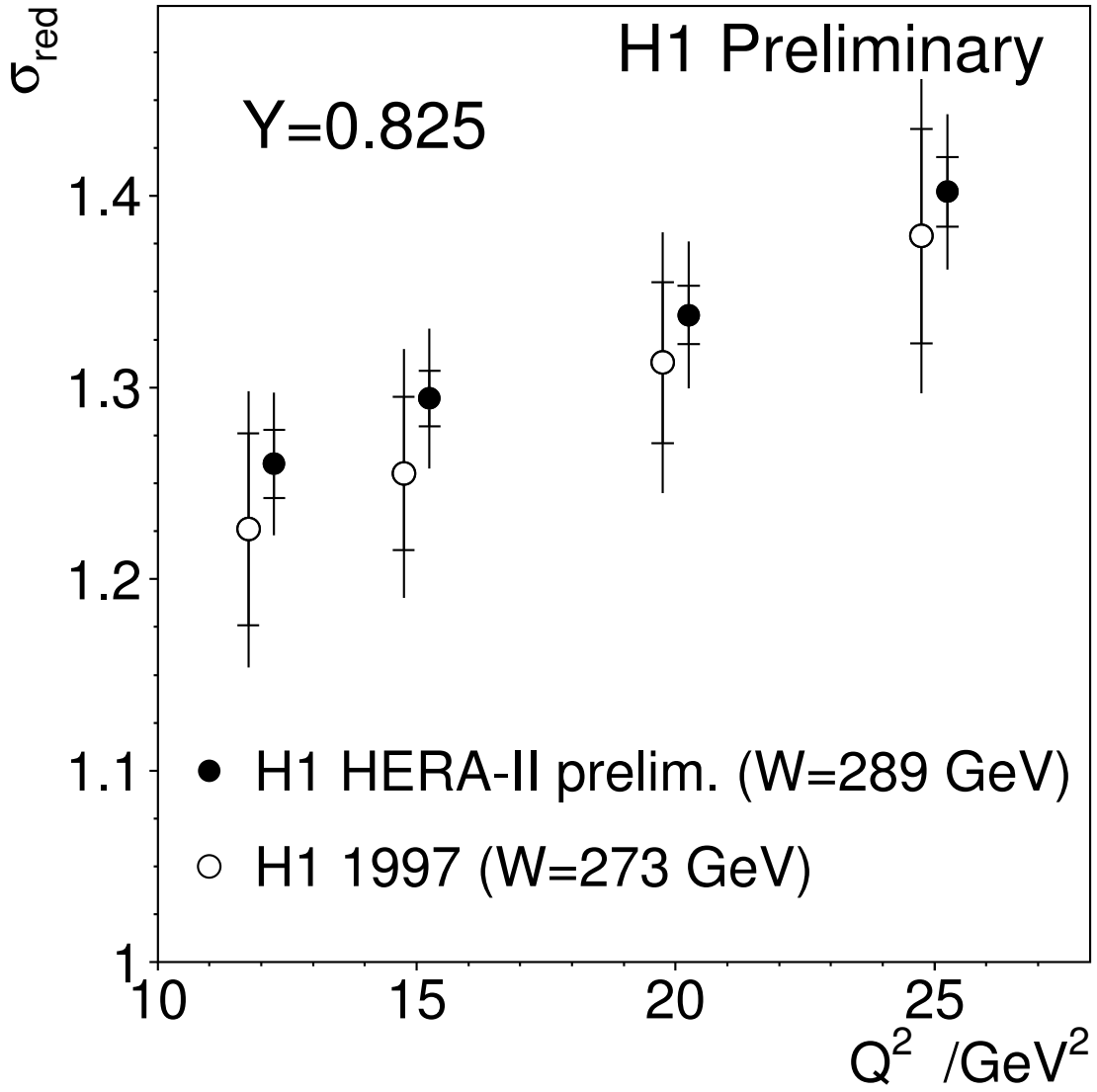

Figure 8: Q^2 dependence of preliminary cross section measurement (solid circles) at inelasticity $y = 0.825$ and the published H1 result (open circles) [7]. Note that the published data corresponds to a slightly lower center of mass energy.

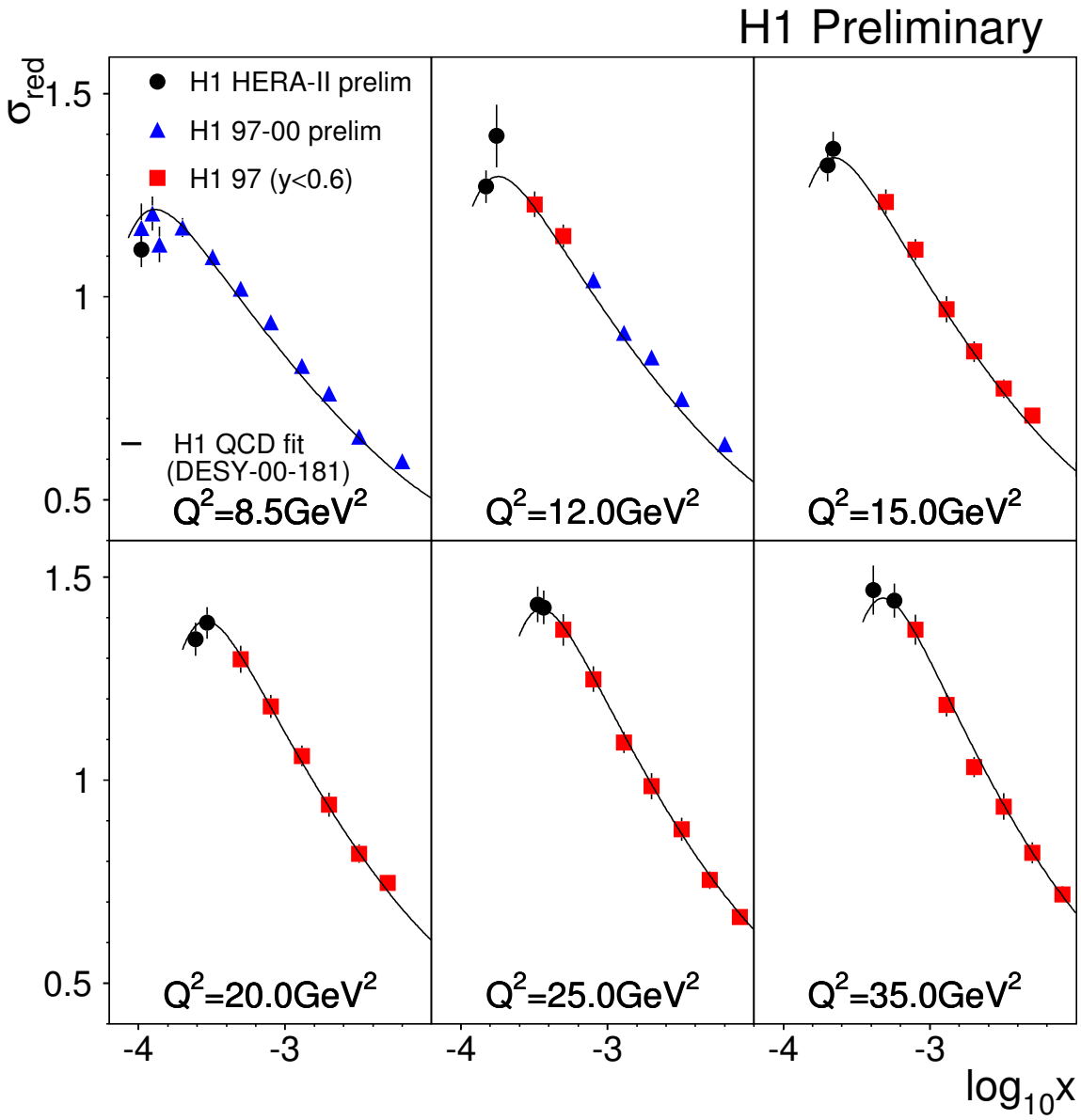

Figure 9: x dependence of the reduced cross section. The measurement presented in this note (circles) with other H1 measurements: a combination of preliminary minimum bias 97 data, minimum bias 99 data and shifted vertex 2000 data (triangles) [8], and measurement from 97 data for $y < 0.6$ (squares) [7]. The line is H1 QCD fit [7]

.